

Nanog Regulates Proliferation During Early Fish Development

ESTHER CAMP,^a ANA V. SÁNCHEZ-SÁNCHEZ,^a ANTONIO GARCÍA-ESPAÑA,^b ROB DESALLE,^c LINA ODQVIST,^a JOSÉ ENRIQUE O'CONNOR,^d JOSÉ L. MULLOR^a

^aDepartment of Regenerative Medicine, Centro de Investigación Príncipe Felipe, Valencia, Spain; ^bResearch Unit, Hospital Universitario de Tarragona Juan XXIII, Instituto Investigaciones Sanitarias Pere Virgili, Tarragona, Spain; ^cSackler Institute for Comparative Genomics, American Museum of Natural History, New York, New York, USA; ^dLaboratory of Cytomics, Mix Research Unit, Centro de Investigación Príncipe Felipe, University of Valencia, Valencia, Spain

Key Words. Nanog • Proliferation • Differentiation • Medaka

ABSTRACT

Nanog is involved in controlling pluripotency and differentiation of stem cells in vitro. However, its function in vivo has been studied only in mouse embryos and various reports suggest that *Nanog* may not be required for the regulation of differentiation. To better understand endogenous *Nanog* function, more animal models should be introduced to complement the murine model. Here, we have identified the homolog of the mammalian *Nanog* gene in teleost fish and describe the endogenous expression of *Ol-Nanog* mRNA and protein during medaka (*Oryzias latipes*)

embryonic development and in the adult gonads. Using medaka fish as a vertebrate model to study *Nanog* function, we demonstrate that *Ol-Nanog* is necessary for S-phase transition and proliferation in the developing embryo. Moreover, inhibition or overexpression of *Ol-Nanog* does not affect gene expression of various pluripotency and differentiation markers, suggesting that this transcription factor may not play a direct role in embryonic germ layer differentiation. *STEM CELLS* 2009;27:2081–2091

Disclosure of potential conflicts of interest is found at the end of this article.

INTRODUCTION

Embryonic stem cells (ESC) are pluripotent and have the capacity to grow indefinitely and differentiate into all cell types of the organism. The homeodomain (HD) transcription factor (TF) *Nanog* is a key regulator of pluripotency in ESC [1, 2]. It acts in conjunction with POU Oct4/Pou5f1 [3] and Sox2 [4] to maintain pluripotency as the core TF triumvirate [5]. In recent years, other proteins have been discovered to participate in this initial triad, such as LIF/gp130/Stat3 in mouse stem cells [6], FoxD3 [7], Sall4 [8–10] and Dax1 [11]. However, *Nanog* is the only one that can replace the need for leukemia inhibitory factor (LIF) in mouse ESC cultures to maintain cell pluripotent characteristics without the apparent need for other factors [1, 2].

A complete lack of *Nanog* causes lethality of murine knockout (KO) embryos [1]. On the other hand, overexpression results in LIF-independent self-renewal of ESC without loss of pluripotent state [2]. However, *Nanog* has a mosaic expression pattern in ESC cultures and cells lacking *Nanog* expression not only maintain an undifferentiated morphology, but can also generate *Nanog*-positive cells [12]. In fact,

Nanog null cells self-renew, are pluripotent and contribute to all somatic tissues, except the gonads, when injected into mice [12]. These in vivo results suggest that *Nanog*'s role in the pluripotency TF triumvirate may be limited to regulating the efficiency of self-renewal. However, after cell fusion of ESC and neural stem cells, the latter adopt a pluripotency state through the action of *Nanog*, which suggests that pluripotency is also conferred by *Nanog* [13]. Additionally, *Nanog* is expressed in the developing gonads of mice and chicken [2, 14–16] and is necessary for murine germ cell development [12], although the functional role of *Nanog* in the developing gonad is unknown.

The regulation of pluripotency by *Nanog*, *Oct4*, and *Sox2* has been described in mammals. However, in vivo functional analysis has been limited to the mouse model. To further understand the in vivo role of pluripotency genes and their regulation, new animal models should be introduced. Recently, both *Oct4* and *Nanog* have been described in chicken [15, 16]. The function of *cNanog* has been characterized in cultured chicken ESC and in mouse ESC, showing that both chicken and mouse *Nanog* share functional homology and that the mammalian pluripotency network also functions in nonmammalian vertebrates. This was confirmed by

Author contributions: E.C., A.V.S.S.: designed and performed research; E.C., A.V.S.S.: collection of data; E.C., A.V.S.S., J.L.M.: data analysis and interpretation; E.C., A.V.S.S., A.G.-E., J.L.M.: manuscript writing; A.G.-E.: designed and performed sequence analysis; R.D.: performed phylogenetic analysis; L.O.: cloned the *Ol-nanog* sequence; J.E.O.: performed flow cytometric data analysis and interpretation; J.L.M.: conception and design, financial support. E.C. and A.V.S.S. contributed equally to this work.

Correspondence: José L. Mullor, Ph.D., Department of Regenerative Medicine, Centro de Investigación Príncipe Felipe (CIPF), Valencia 46012, Spain. Telephone: +34 963 289 680; Fax: +34 963 289 701; e-mail: jmullor@cipf.es Received February 12, 2009; accepted for publication May 9, 2009; first published online in *STEM CELLS EXPRESS* May 21, 2009. © AlphaMed Press 1066-5099/2009/\$30.00/0 doi: 10.1002/stem.133

studies in *Xenopus*, in which three *Oct4* homologs have also been described; one of them, *XIPou91*, shares functional similarity with mammalian *Oct4* in maintaining stemness during early development [17]. In addition, self-renewing ES-like cells from zebrafish and medaka have been characterized [18, 19]; *Oct4*-like sequences have been identified in medaka *Ol-pou5f1* [20] and zebrafish *pou2/spg* [21]. Furthermore, in vitro analysis has demonstrated that the murine *Oct4* promoter is activated in medaka ESC, suggesting that the pluripotency regulatory network is conserved in fish [22]. Thus, in addition to their favorable experimental characteristics, fish are an excellent model to study the role of Nanog and pluripotency during vertebrate development.

In this study, we have identified *Nanog* homologs in various species, including the *Ol-Nanog* homolog in medaka. We describe *Ol-Nanog* endogenous mRNA and protein expression during embryonic development and in adult gonads for the first time in teleost fish. Using mRNA and morpholino (MO) microinjections for gain- and loss-of-function experiments, we show that *Ol-Nanog* is required for S-phase transition and proliferation during early embryonic development, without having an effect during early germ layer differentiation.

MATERIALS AND METHODS

Fish Embryos

Adult medaka CAB strain animals were kept in recirculating water aquaria at 26°C on a 14-hour light/10-hour dark daily cycle. Embryos were collected by natural spawning in Yamamoto solution (0.13M NaCl, 2.7 mM KCl, 1.8 mM CaCl₂, and 0.24 mM NaHCO₃; pH 7.3) [23] and staged as previously described [24]. Embryos were raised at 25°C.

Data Mining and Sequence Analysis

Blast searches were performed searching the various genome-sequencing projects with the Blast-T program with multiple starting queries using the National Center for Biotechnology Information (<http://www.ncbi.nlm.nih.gov>) and the Ensembl (<http://www.ensembl.org>) servers. Intron-exon borders were determined with the NCBI Blast program (<http://www.ncbi.nlm.nih.gov>). Alignments of protein sequences were performed using the ClustalW or the Multialign programs from the Network Protein Sequence Analysis (http://npsa-pbil.ibcp.fr/cgi-bin/npsa_automat.pl?page=/NPSA/npsa_server.html). Identities and similarities between protein sequences were calculated with the Dialign software from the Genomatix suite (<http://www.genomatix.de/cgi-bin/dialign/dialign.pl>). Diagnostic characters were determined as previously described [25]. The phylogenetic analysis was generated with PAUP* (version 4.0; Sianuer Associates, Inc., Sunderland, MA, <http://www.paup.csit.fsu.edu/>) [26] using the HD amino acid sequences. We used the Jackknife resampling procedure in PAUP* to generate jackknife proportions for the nodes in the tree. The tree searches were heuristic with 100 random additions and TBR branch swapping in each replicate for 1,000 replicates.

Polymerase Chain Reaction Analysis

Total RNA was extracted from groups of 20 embryos at the appropriate stage using Trizol reagent (Sigma-Genosys, Cambridge, U.K., http://www.sigmaaldrich.com/Brands/Sigma_Genosys.html) and treated with DNA-free kit (Applied BioSystems, Foster City, CA, <http://www.appliedbiosystems.com>). cDNA were synthesized from 1 µg of total RNA using random primer hexamers (Roche Diagnostics, Basel, Switzerland, <http://www.roche-applied-science.com>) and Superscript III reverse transcriptase (Invitrogen, Carlsbad, CA, <http://www.invitrogen.com>) from two independent experimental groups of treated embryos. Equal amounts of cDNA were amplified in triplicate using specific

primer pairs (supporting information Table 5). The annealing temperature used for all primer pairs was 57°C. To perform semi-quantitative analysis, the number of cycles was optimized by determining the exponential range of amplification for each primer pair, except where noted. A negative control to confirm the absence of gDNA was performed using *Actin* primers on RNA without reverse transcriptase (RT). Polymerase chain reaction (PCR) analysis was performed in triplicate in two different injection experiments.

For quantitative RT (qRT)-PCR, we used 1.7 ng of cDNA in 1× SYBR Green Master Mix (Bio-Rad, Hercules, CA, <http://www.bio-rad.com>) and 0.25 mM each forward and reverse primers (supporting information Table 5). The PCR amplification and fluorescence detection were performed in a real-time PCR thermal cycler (MiniOpticon, Bio-Rad). The PCR conditions were 35 cycles of denaturation at 95°C for 15 seconds, annealing for 58°C for 45 seconds, and extension for 30 seconds at 72°C. The melting curve was constructed by plotting fluorescence data against temperature (55°C–95°C). Control samples without cDNA were included in all assays to confirm the absence of nonspecific amplification products. For each sample, the threshold cycle (C_t) for the internal control (*Actin*) amplification was subtracted from the threshold cycle of the corresponding transcription factor amplification (C_t, transcription factor) to yield ΔC_t. The Pfaffl method was used to calculate the ratio of relative gene expression related to *Actin* (internal control) and is represented in the bar graphs. Primer pair efficiencies were calculated for each primer pair by performing dilution curves (*CcnD1*:1.92, *CcnA*:1.95, *Actin*:1.99). qRT-PCR reactions were performed in triplicate for each experiment. Bar graphs represent the results from six independent experiments performed on cDNA samples from two different treated groups of embryos (three experiments per sample).

mRNA and Morpholino Injection

The *Ol-Nanog* cDNA was amplified using the following primers: Nanog F, ATGGCGGAGTGGAAAACCTC; NanogR, TCATTG-GACAGCATTGTGC. It was cloned in *pCS2+* and *pCS2+MT*. *pCS2+Ol-Nanog*, *pCS2+MT-Ol-Nanog*, *HSGFP3* (from T. Czerny, Wien, Austria) were used for mRNA synthesis with the SP6 mMessage mMachine Kit (Ambion, Austin, TX, <http://www.ambion.com>). The MO (Gene Tools, Philomath, OR, <http://www.gene-tools.com>) sequences were *ATG MO 5'-TGACCTGAG TTTTCCACTCCGCCAT-3'*, *ile2 MO 5'-TCCAAGAATCTGTT GAGGGAATGAA-3'*, and control MO (*MO-C*) *5'-CCTCTTACC TCAGTTACAATTTATA-3'*. MOs or synthesized mRNAs were injected in CAB embryos at stage 2 using a pressure Narishige IM300 microinjector (Narishige, London, UK, <http://uk.narishige-group.com/>).

Immunohistochemistry

The medaka-specific anti-*Ol-Nanog* antibody was raised in rabbits (Abnova) against the peptide sequence GGENTRRTGSDSASD-SEAH. Anti-*Ol-Nanog* was used at 1:200, anti-Myc (no. OP10L; Calbiochem, San Diego, CA, <http://www.emdbiosciences.com>) at 1:500 and anti-phospho-histone H3 (anti-pH3) at 1:200 (no. 9701; Cell Signaling Technology, Beverly, MA, <http://www.cellsignal.com>) in embryos fixed at desired stages in 4% paraformaldehyde/1× phosphate buffer saline Tween (PBSTw). For anti-*Ol-Nanog* staining, embryos were first boiled in 10 mM sodium citrate buffer (pH 6.0) for 5 minutes. Embryos were incubated with Alexa488-conjugated anti-rabbit (no. A11008, Invitrogen) or Cy3-conjugated anti-rabbit (no. 111-166-045, Jackson Immuno-research Laboratories, West Grove, PA, <http://www.jacksonimmuno.com>) at 1:500 and 4',6-diamidino-2-phenylindole (DAPI). Finally, all embryos were mounted using fluoromount G medium.

The number of DAPI- and pH3-positive cells was counted from four sectors of equal size in each injected embryo and analyzed using GraphPad Prism (GraphPad Software Inc) and *t* test or one-way analysis of variance plus Tukey post hoc test analysis (*p* < .05). Whole and 10-µm cryosections of adult gonads were

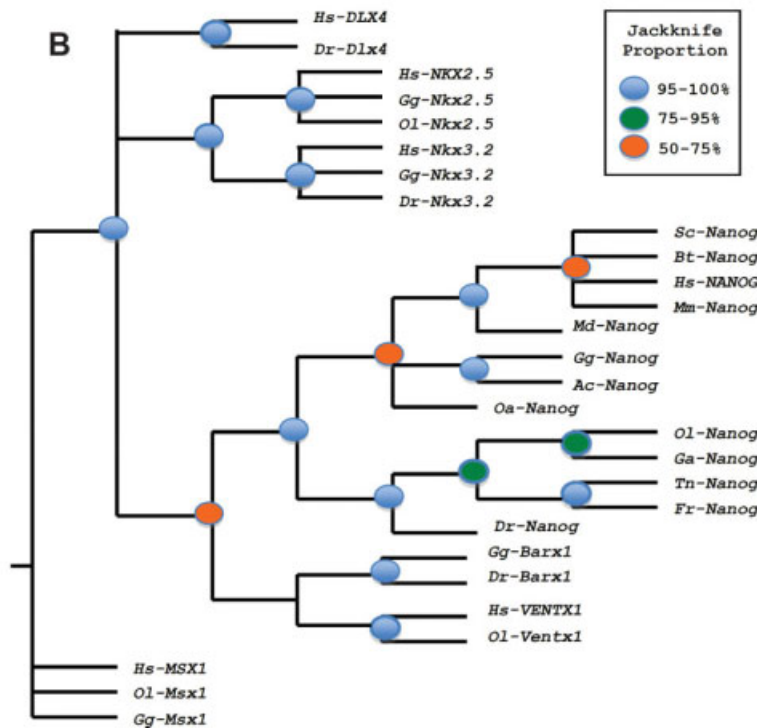


Figure 1. Comparative analysis of Nanog and Nanog-like protein sequences. (A): Alignment of the homeodomain (HD) protein regions of Nanog and Nanog-like proteins from fish, tetrapods, and closely related HD proteins. The alignment is shaded with respect to the medaka protein, with the percentage of similarity to medaka shown on the right; orange, identical in all sequences; green, identical; yellow, similar to medaka. HD residues are conventionally numbered 1-60 (residues 95-154 of human Nanog). Red asterisks mark the Nanog HD specific amino acids. (B): Phylogenetic tree analysis using the amino acid sequences from the HD. Abbreviations: Ac, *Anolis carolinensis*; Bt, *Bus taurus*; Dr, *Danio rerio*; Fr, *Fugu rubripes*; Ga, *Gasterosteus aculeatus*; Gg, *Gallus gallus*; Hs, *Homo sapiens*; Md, *Monodelphis domestica*; Mm, *Mus musculus*; Oa, *Ornithorhynchus anatinus*; Ol, *Oryzias latipes*; Sc, *Sus scrofa*; Tn, *Tetraodon nigroviridis*.

stained for anti-Ol-Nanog following the above immunostaining instructions. Control immunofluorescence experiments were performed using either preimmunization serum (preserum), or secondary antibody alone, or preadsorbed Nanog antibody with the immunogenic peptide. Preadsorption of the Nanog antibody with the immunogenic peptide was performed at an antibody-to-peptide ratio of 1:20 mol in 1% bovine serum albumin and phosphate-buffered saline, and was incubated overnight at 4°C with rotation. The treated solution was then used as primary antibody in immunohistochemistry experiments. Images were obtained with a Leica MZ16FA stereomicroscope, Leica DM5000B fluorescent microscope, and confocal images with a Leica DM IRE2 microscope (Leica, Heerbrugg, Switzerland, <http://www.leica.com>). Hematoxylin and eosin staining of testes cryosections were performed as previously described [27].

Whole Mount In Situ Hybridization

The *Ol-Nanog*, *Ol-Oct4*, *Ol-Bra*, and *Ol-Pax6* RNA probes were synthesized following standard protocols. The *Oct4* gene was

amplified and cloned in pCS2+ using the primers: Oct4F, ATGTCTGACAGGCCGCAC; Oct4R, ATCCTGTGAGGTGACCTA. Whole mount in situ hybridization (WMISH) was performed as described [28] on embryos fixed with 4% paraformaldehyde/2× PBSTw at the desired stages or adult gonads before cryosections (35 μm).

Cell Cycle Analysis

Cells were extracted from live *MO-C* or *MO-Nanog* injected embryos (three independent experiments) at stage 16 and trypsinized (trypsin/EDTA 25200-072, Invitrogen). Cell suspension was centrifuged, washed with phosphate-buffered saline, and fixed with 70% ethanol overnight at -20°C. For flow cytometric determination of DNA content in single cells, cell pellets were resuspended in 300 μl propidium iodide solution containing propidium iodide (50 μg/ml) and RNase A (10 μg/ml) and stained overnight at 4°C. Cell suspensions were analyzed in a Cytomics FC500 flow cytometer (Beckman Coulter, Fullerton, CA, <http://www.beckmancoulter.com>). For calculation of cell size and fitting

cell cycle phases from the primary cytometric data, the public domain software WinMDI 2.8 (<http://facs.scripps.edu/software.html>) and Cylchred (<http://www.facs-lab.toxikologie.uni-mainz.de/engl-1.%20Websites/Downloads-engl.jsp>) were used, respectively. Experiments were performed and analyzed using GraphPad Prism (GraphPad Software, La Jolla, CA, <http://www.graphpad.com>) and *t* test analysis ($p < .05$).

RESULTS

Identification of Nanog Related Proteins in Fish

We used known Nanog protein sequences from mammals as query to perform blast searches in representative vertebrate sequenced genomes. This approach yielded Nanog-like sequences in several species, including medaka fish (Fig. 1 and supporting information Table 1). Analysis of the intron/exon gene structure can help determine the evolutionary conservation or origin of a gene family [29]; thus, we analyzed the intron/exon gene structure of the sequences. In all Nanog and Nanog-like sequences (except in humans), we observed conservation of the location and phase of the first intron (at the amino terminal region and in phase 1, between the first and second bases of the codon). We also observed conservation of phase 0 (between codons) of the second and third introns (supporting information Figs. 2 and 3). Thus, the identified nonmammalian Nanog-like sequences share the intron/exon gene structure with mammalian sequences. In addition, all Nanog and Nanog-like sequences have an amino terminal conserved serine-rich region (e.g., 18.3% serines in humans, 17.5% in chicken, and 18.4% in medaka; supporting information Fig. 4).

Alignment of Nanog and Nanog-like protein sequences showed an expected low sequence conservation (supporting information Table 2). However, sequence conservation in the HD was more pronounced (supporting information Fig. 1A and supporting information Table 3). The HD region characterizes and defines the different homeobox proteins and, consequently, the amino acids implicated in the preservation of the structural integrity of the HD (Asn51, Arg53, Leu16, Phe20, Val45, Trp48 and Phe49, following conventional HD numbering) are conserved in all Nanog-like HD. A comparison of the HD region shows that tetrapod Nanog HDs are more similar to fish Nanog HD than to other protein HD (Fig. 1A). Moreover, there are four specific Nanog HD residues (Met31, Tyr42, Lys43, Thr47) that differ from other HDs and which confer the Nanog HD its binding specificity [30]. These residues are also conserved in fish Nanog-like sequences (Fig. 1A). Moreover, we found that Met31 is conserved between fish, human and mouse, but not other tetrapods. Thus, our *in silico* analysis shows conservation of the intron/exon genomic structure, the serine-rich domain, the HD sequence, and the specific Nanog amino acids.

To further analyze the similarities between mammalian and fish *Nanog*, we performed a synteny analysis of the *Nanog* gene in fish and human genomes. Initially, our analysis showed that there is only one copy of *Nanog* in medaka on chromosome 20. Previous whole genome orthology analysis also suggested a single copy of a putative medaka ortholog of human *Nanog* on chromosome 20 [31]. We also identified one copy of *Nanog* in other teleost fish (zebrafish, puffer fish, and stickleback). Results from the synteny analysis showed that synteny around the human *Nanog* gene is lost in fish. The synteny around the fish *Nanog* is conserved in mammals; however, the intergenic region between *Nanog*'s flanking genes (*IPO4* and *TM9SF1*) is smaller than in fish (287 bp in mouse, 1,298 bp in human, and 602 bp in the marsupial opos-

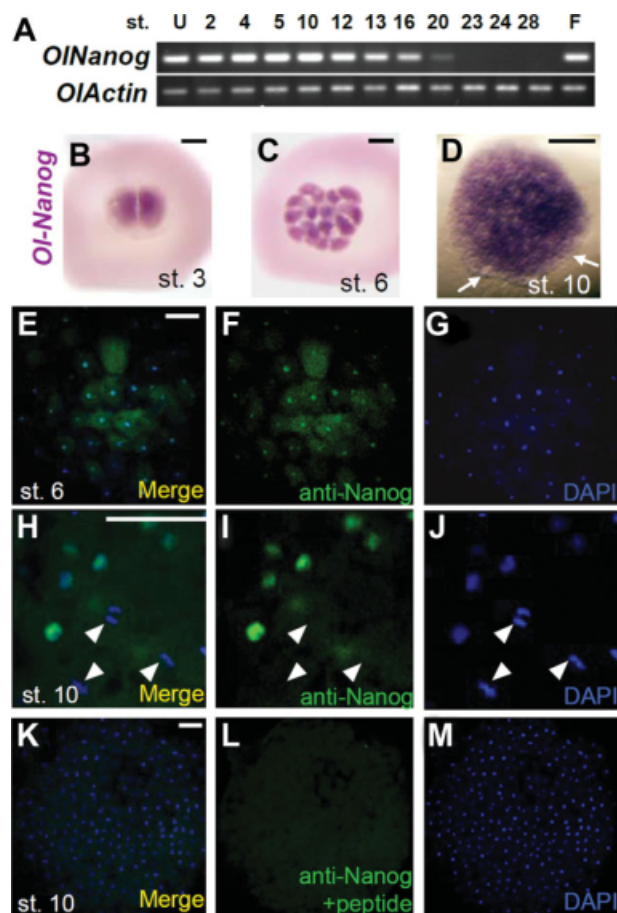


Figure 2. Expression of OI-Nanog in medaka. (A): Reverse-transcriptase polymerase chain reaction (RT-PCR) analysis of *OI-Nanog* mRNA at different developmental stages. The RT-PCR number of cycles was 35. (B–D): *OI-Nanog* WISH. Arrows mark marginal cells. Scale bars = 200 μ m. (E–M): Immunofluorescence showing anti-Nanog protein expression. Blastomeres show OI-Nanog predominantly in nuclei and are evenly dispersed in the cytoplasm during cell division (arrowheads). (K–M): Control immunohistochemistry experiment using preabsorbed OI-Nanog showing no signal. Scale bars = 50 μ m. Abbreviations: F, fry; U, unfertilized eggs.

sum, whereas in fish it ranks between 4,940 bp in medaka and 8,750 bp in stickleback). This suggests a putative deletion or transposition event in the region between these genes in mammals. We therefore considered the synteny analysis to be nondeterminant with respect to establishing orthology of the fish *Nanog* to the mammal *Nanog*.

Because the synteny analysis was nondeterminant and as the amino acid similarity was not enough to claim orthology, we performed further sequence analysis using the diagnostic amino acid approach [25] to determine orthology. We first established an alignment of the homeobox region of several proteins closely related to the Nanog family in several organisms. We used this alignment to establish diagnostics for the six major homeobox families in our data set (supporting information Fig. 5). This analysis demonstrated that there are eight diagnostics in the potential fish Nanog HD, four of which are found in Nanog from other species (supporting information Fig. 5, indicated by blue bars below the sequences). As for the other four diagnostics, each represents single diagnostic matches with the other homeobox families analyzed (*Barx*, *Dlx*, *Msx*, and *Ventx*). Furthermore, we also performed a

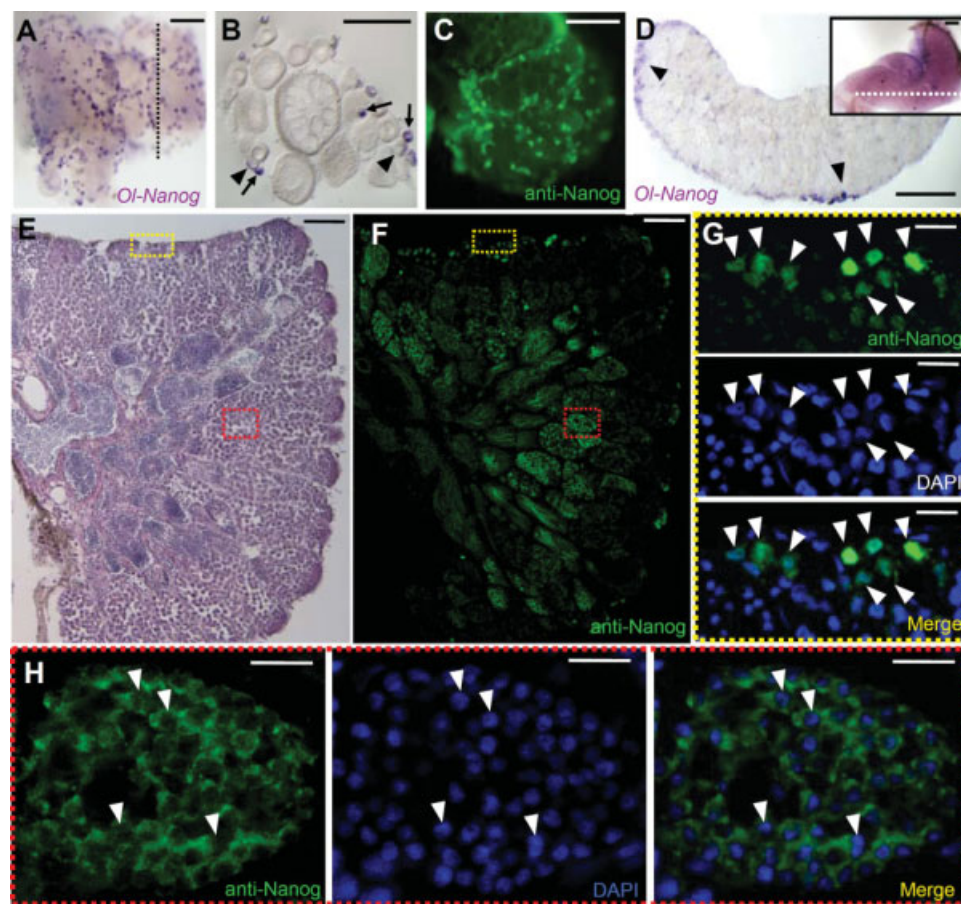


Figure 3. Expression of *Ol-Nanog* in gonads. (A–C): Whole mount in situ hybridization and immunohistochemistry to detect *Ol-Nanog* in whole and sectioned ovaries. Scale bars = 100 μm . (B): Section taken from (A) showing small previtellogenic oocytes (arrows) that express high levels of *Ol-Nanog*. As they grow, *Ol-Nanog* expression is diminished (arrowheads). (D): *Ol-Nanog* WMISH in whole and sectioned testis. Expression is detected mainly in the periphery of the testis where the spermatogonia are located (arrowheads). Scale bars = 100 μm . (E): Hematoxylin-Eosin stain of medaka testis. (F–H): *Ol-Nanog* expression in testis sections. Scale bar in (F) = 50 μm . (G): Magnified insert from (F), in which *Ol-Nanog* is detected in the nucleus of cells in the periphery (arrowheads). Scale bars = 10 μm . (H): Magnified insert from (F), in which *Ol-Nanog* is detected only in the cytoplasm of cells within cysts and not in the nucleus (arrowheads). Scale bars = 10 μm .

phylogenetic analysis using the HDs of these proteins, as recent approaches to establishing orthology also used phylogenetic approaches [32]. The phylogenetic tree (Fig. 1B) demonstrates that the potential fish *Nanog* orthologs are clearly more evolutionary related to the mammalian *Nanog* orthologs from other vertebrates than they are to any of the other homeobox domains in the analysis. The results from all our sequence analysis strongly suggest that the potential fish genes are indeed orthologs of *Nanog*.

***Ol-Nanog* Expression During Medaka Development and in Adult Gonads**

To functionally characterize the medaka *Nanog* gene, *Ol-Nanog*, we first cloned and sequenced the predicted gene sequence using RT-PCR on cDNA synthesized from a pool of medaka embryos at different developmental stages (GenBank accession FJ436046). The expression pattern of *Ol-Nanog* was examined by RT-PCR (Fig. 2A) and WMISH (Fig. 2B–2D). We found that in contrast to the mouse, where *Nanog* is first detected in the embryo at the morula stage [2], *Ol-Nanog* was observed to be maternally inherited and mRNA expression could be detected in the unfertilized egg, the two-cell stage embryo (Fig. 2A, 2B) and throughout early development until stage 20 (optic cup stage; Fig. 2A). At stage 10, *Ol-Nanog* spatial expression remained in the majority of blastomeres; however, it was absent in the marginal cells (Fig. 2D). After stage 20, *Ol-Nanog* expression was not detected until later in development, during the early fry stage (Fig. 2A).

To study protein expression and subcellular localization, we generated a polyclonal antibody specific for medaka *Ol-Nanog*. For control experiments to determine antibody speci-

ficity, we used serum from the rabbit before immunization (pre-serum), *Ol-Nanog* antibody pre-adsorbed with the immunogenic peptide (see Materials and Methods) or only the secondary antibody. Fluorescent immunohistochemistry with these reagents showed no specific staining (Fig. 2K–M and supporting information Fig. 6). *Ol-Nanog* protein was detected predominantly in the cell nucleus of early-stage embryos, although some staining was observed in the cytoplasm (Fig. 2E–J). Moreover, during cell divisions, as detected by DAPI staining of mitotic chromosomes, *Ol-Nanog* was evenly dispersed in the cytoplasm (Fig. 2H–J).

In mice, *Nanog* is expressed in primordial germ cells (PGC), the genital ridges, and the developing gonads [2, 14]; in chickens, expression has been detected in the developing gonads [15, 16]. Thus, we evaluated the presence of *Ol-Nanog* in the medaka gonads. *Ol-Nanog* mRNA and protein expression were detected in male and female gonads. In the ovary, the *Ol-Nanog* gene and protein were present only in the small previtellogenic oocytes and the signal diminished and was undetectable in medium to large previtellogenic oocytes (Fig. 3A–C). In testes, *Ol-Nanog* gene expression was detected in the peripheral zone corresponding to the layer of spermatogonia (Fig. 3D). We combined Hematoxylin-Eosin staining to visualize tissue structure and immunofluorescence to detect *Ol-Nanog* protein expression on testis cryosections. *Ol-Nanog* was detected in the nucleus of cells in the most peripheral region of the testis where spermatogonia are located (Fig. 3E–G) and in the cytoplasm of cells located within cysts in which spermatogenesis takes place (Fig. 3E, 3F, 3H). These results demonstrate that *Nanog* is expressed in the developing fish embryos and the adult gonads.

Ol-Nanog Is Necessary for Correct Embryonic Development

We generated specific MOs, which block mRNA translation, against *Ol-Nanog* for loss-of-function studies and used *Ol-Nanog* mRNA tagged with the *myc* epitope for gain-of-function studies. We depleted the levels of the Ol-Nanog protein using two different MOs: one against the ATG sequence (*ATG MO*) and another against the intron1-exon2 junction (*ile2 MO*). Embryos injected with control MO (*MO-C*) developed normally. At stage 16, the blastula of *MO-C* injected embryos covered three quarters of the yolk sphere and the embryonic shield appeared as a narrow streak (Fig. 4A); at stage 23, head structures and somites were clearly visible (Fig. 4D). In contrast, injection of both the *ATG MO* and the *ile2 MO* caused an abnormal phenotype in stage 16 embryos (Table 1). The blastula of these embryos covered only half of the yolk and the developing embryonic shield appeared as a dense, compacted mass of large cells (Fig. 4B). When observed at the same time as stage 23 control embryos, these embryos were reduced in size and constituted a compacted mass of large cells without head or tail structure development (Fig. 4E). This phenotype produced developmental arrest and embryonic death. The two MOs designed against *Ol-Nanog* produced the same phenotype, although *ATG MO* affected a greater percentage of embryos than *ile2 MO* (Table 1). Thus, in subsequent experiments, we only used the *ATG MO*, referred to as *MO-Nanog*.

To test whether the phenotype of *MO-Nanog* injected embryos was specific for the depletion of Ol-Nanog protein, we first analyzed Ol-Nanog protein levels in vivo after *MO-Nanog* injection (Fig. 4H–K). Immunohistochemistry on *MO-Nanog* injected embryos confirmed the loss of Ol-Nanog localization in the nucleus (Fig. 4J, 4K). Additionally, we coinjected *MO-Nanog* with *Ol-Nanog myc*-tagged mRNA at different concentrations to perform rescue studies. Coinjections resulted in moderate to complete rescue of the *MO-Nanog* phenotype and embryonic viability by the *Ol-Nanog* mRNA (Fig. 4O–Q). Moderate or complete rescue was dependent on the mRNA concentration co-injected (supporting information Table 4). The lower concentration of *Ol-Nanog* mRNA (100 ng/ μ l) resulted in 52% complete rescue and 40% moderate rescue ($n = 108$), whereas the higher concentration (200 ng/ μ l) resulted in 85% complete rescue and 15% moderate rescue ($n = 116$; supporting information Table 4). Hence, these results confirm that the *MO-Nanog* phenotype was due specifically to depletion of endogenous *Ol-Nanog* mRNA.

As the rescue experiments show, our synthetic *Ol-Nanog* mRNA was functional and able to rescue the lack of endogenous *Ol-Nanog* function. However, when overexpression experiments were performed using two different concentrations of *Ol-Nanog* mRNA, no specific phenotypes were detected (Fig. 4C, 4F, 4G, Table 1). Using fluorescent immunohistochemistry to detect the *myc*-epitope attached to the *Ol-Nanog* mRNA, we detected the recombinant Ol-Nanog protein in the nucleus of cells from *Ol-Nanog* mRNA injected embryos (Fig. 4L–N). Thus, overexpression of a functional Ol-Nanog protein, which localized to the nucleus, did not alter normal development of medaka embryos.

Ol-Nanog Is Necessary for Cell Proliferation and the Correct Transition Through S Phase

To characterize the phenotype of Nanog-morphant embryos, we first focused on cell proliferation as *MO-Nanog* injected embryos presented fewer and larger cells than the controls. This observation was quantified by counting the number of DAPI-stained nuclei in squares of a fixed area (sectors). *MO-Nanog* injected embryos contained fewer nuclei per sector

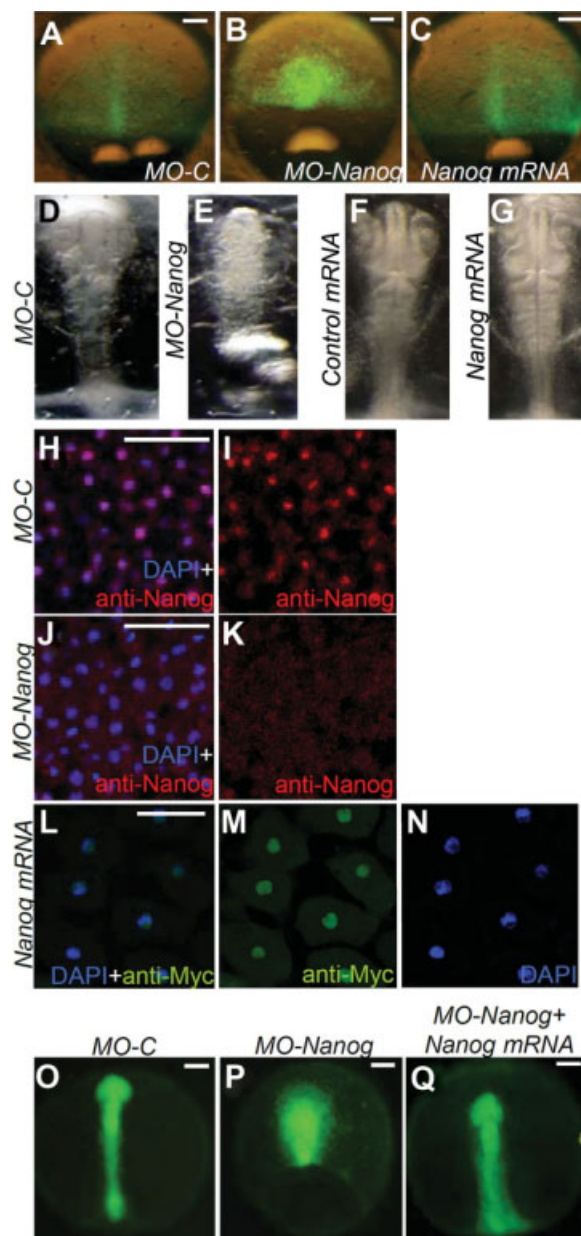


Figure 4. *Ol-Nanog*-specific morpholino (MO) alters early development, but *Ol-Nanog* gain of function does not induce a phenotype. (A–C): Embryonic phenotypes 24 hours after injection of *MO-C*, *MO-Nanog*, or *Ol-Nanog* mRNA. GFP mRNA was coinjected as cell tracer. Scale bars = 200 μ m. (D–G): Phenotype induced after *Ol-Nanog* depletion or overexpression in stage 23 embryos. (H–K): *Ol-Nanog* in the nucleus is lost in *MO-Nanog* injected embryos. The results represent three independent experiments with a total of $n = 28$ (*MO-C*) and $n = 33$ (*MO-Nanog*). Scale bars = 50 μ m. (L–N): *Myc*-tagged *Ol-Nanog* mRNA produces a protein that is localized in the nucleus as endogenous *Ol-Nanog*. The results represent two independent experiments with total $n = 26$. Scale bars = 25 μ m. (O–Q): *Ol-Nanog* mRNA coinjection with *MO-Nanog* rescues the MO-induced phenotype. Scale bars = 200 μ m.

(19.69 ± 1.31 , total $n = 15$ from three different experiments) compared with *MO-C* injected embryos (34.58 ± 2.62 , total $n = 15$ from three different experiments; Fig. 5A, 5B, 5E) and the cells appeared to be larger (Fig. 4A, 4B), suggesting that proliferation may be compromised. We assayed for

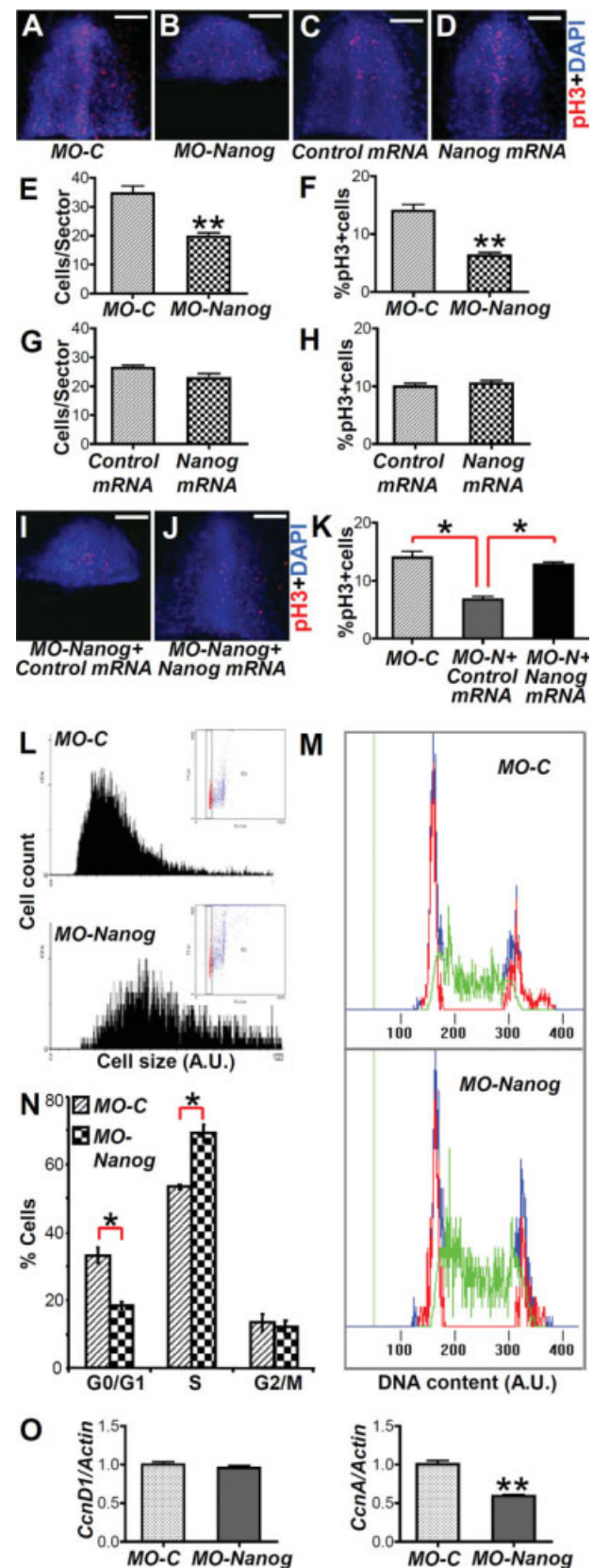
	Concentration	Nanog-specific phenotype (%)	Normal (%)	n
MO-C	1 mM	0	75	166
	0.5 mM	0	81	111
ATG MO (MO-Nanog)	1 mM	88	2	161
	0.5 mM	77	14	138
i1e2 MO	0.5 mM	39	41	88
Control mRNA	100 ng/ μ l	0	71	126
	200 ng/ μ l	0	78	176
Nanog mRNA	100 ng/ μ l	0	79	126
	200 ng/ μ l	0	76	137
	400 ng/ μ l	0	78	81

Nonspecific phenotypes (i.e., injection phenotypes) are not represented in the table, but represent the difference between the reported values and 100%. Each experiment was performed in triplicate and n represents the total number of embryos from the three experiments.

proliferation using a pH3 antibody as a marker of proliferating cells in M phase. At stage 16, *MO-C* injected embryos contained $14.0 \pm 1.1\%$ (total $n = 15$ from three different experiments) pH3-positive cells, whereas only $6.3 \pm 0.5\%$ (total $n = 15$ from three different experiments) cells were pH3-positive in *Nanog*-morphant embryos (Fig. 5F). However, overexpression of *Ol-Nanog* mRNA had no effects on cell number or percentage of pH3-positive cells when compared to the control (Fig. 5C, 5D, 5G, 5H). Rescue studies were performed to determine if the proliferation defect seen in *MO-Nanog* injected embryos could be rescued by *Ol-Nanog* mRNA. Co-injection of *MO-Nanog* with *Ol-Nanog myc*-tagged mRNA at 200 ng/ μ l resulted in an increase in the percentage of pH3 positive cells ($12.7 \pm 0.6\%$, total $n = 17$ from two different experiments) when compared with the percentage of pH3-positive cells in embryos co-injected with *MO-Nanog* and *Control mRNA* ($6.7 \pm 0.4\%$, total $n = 11$ from two different experiments, Fig. 5I–K). There was no statistical difference between the percentage of pH3 positive cells of embryos co-injected with *MO-Nanog* and *Ol-Nanog* mRNA with that of *MO-C* con-

Figure 5. Depletion of *Ol-Nanog* by *MO-Nanog* decreases cellular proliferation in embryos and alters S-phase transition. (A, B, E, F): Cell proliferation assay at stage 16 in *MO-Nanog* injected embryos. The results represent two independent experiments and four sectors per embryo. (C, D, G, H): Cell proliferation assay at stage 16 in *Ol-Nanog* mRNA injected embryos. There is no change in cell number or percentage of pH3-positive cells. The results represent two independent experiments and four sectors per embryo. (I–K): Cell proliferation assay at stage 16 in *MO-Nanog*+*Ol-Nanog* mRNA (rescue experiments) injected embryos. There is a rescue of the *Nanog*-morphant phenotype and an increase in the percentage of pH3-positive cells when compared to *MO-Nanog*+*control mRNA* injected embryos (K). The results represent two independent experiments and four sectors per embryo. *MO-Nanog* was named as *MO-N*. (L): Histogram of cells in G0/G1 phase (insets) from *MO-C* and *MO-Nanog* injected embryos representing cell size. (M): Histograms of cells from *MO-C* and *MO-Nanog* injected embryos demonstrating the distribution and number of cells according to DNA content, which represents the number of cells in each phase of the cell cycle. (N): Bar graphs representing the percentage of cells in G0/G1, S, and G2/M from *MO-C* and *MO-Nanog* injected embryos. The results represent three independent experiments. (O): *CcnD1* and *CcnA* expression detected using qualitative reverse-transcriptase polymerase chain reaction in *MO-C* and *MO-Nanog* injected embryos. Data presented as mean \pm SEM. Scale bars = 200 μ m. Abbreviations: *, $p < .005$; **, $p < .0005$. AU, Arbitrary units.

trol injected embryos, thus *Ol-Nanog* mRNA was able to rescue the proliferation defect observed in *Nanog*-morphant



embryos (Fig. 5K). These results reveal that *OI-Nanog* is required for normal proliferation of early embryonic cells.

To analyze how *OI-Nanog* affects cell cycling properties, cells from *MO-Nanog* and *MO-C* injected embryos at stage 16 were fixed and stained with propidium iodide (PI) for DNA content analysis using flow cytometry. Using this technique, individual cell size can also be measured during the different cell cycle phases. To avoid interference from size changes due to DNA synthesis and cell division, we focused on the histograms of cells at G0/G1 phase. Cell distribution from *MO-Nanog* injected embryos was shifted to larger sizes as compared to control (Fig. 5L), supporting our previous observation of the presence of larger cells in whole embryos. Most importantly, the distribution of cells according to DNA content which represents the number of cells in each phase of the cell cycle showed that there was an increase in the percentage of cells in S-phase in *MO-Nanog* injected embryos ($69.37 \pm 2.40\%$, total $n = 89$ from three different experiments) when compared to *MO-C* injected embryos ($53.39 \pm 0.65\%$, total $n = 94$ from three different experiments). This was accompanied by a decrease in the percentage of cells in G0/G1 phase in *MO-Nanog* injected embryos ($18.43 \pm 1.12\%$, total $n = 89$ from three different experiments) when compared to *MO-C* injected embryos ($33.18 \pm 2.28\%$, total $n = 94$ from three different experiments; Fig. 5M, 5N). In addition, we performed qRT-PCR to detect any changes in the expression of *CyclinD1* (*CcnD1*), an important regulator of cell cycle progression from G1 to S-phase, and *CyclinA* (*CcnA*), which is required for cell progression through the S-phase. In *Nanog*-morphant embryos we observed a decrease in *CcnA* expression, but no change in *CcnD1* expression when compared to the control *MO-C* injected embryos (Fig. 5O). These results indicate that *OI-Nanog* is necessary for S-phase progression and/or exit.

OI-Nanog Does Not Regulate Early Lineage Commitment In Vivo

The embryonic shield in *Nanog*-morphant embryos appeared as a dense group of large cells and did not form a narrow streak, suggesting that *OI-Nanog* depletion may cause defects during cell specification after gastrulation. Expression of early differentiation markers was examined by WMISH for the mesoderm marker *Brachyury* (*Bra*) [33], the ectoderm marker *Pax6* [34], and the pluripotency marker *Oct4* [3]. In *MO-Nanog* injected embryos, the *Bra* gene expression pattern was maintained proportional to the size of the embryo, indicating that mesoderm induction had occurred normally, *Pax6* levels were partially diminished and *Oct4* expression pattern was disorganized, but importantly, all three marker genes were expressed (Fig. 6A–D). Additionally, overexpression of *OI-Nanog* had no effect on marker gene expression patterns or levels (Fig. 6A–D), although higher *OI-Nanog* mRNA levels than in the control could still be detected at st. 16 (Fig. 6E). We reasoned that if *OI-Nanog* was necessary to maintain pluripotency, depletion of this TF would induce early activation of differentiation markers and inhibition of pluripotency markers. However, the activation of differentiation-specific genes occurred at the same stages as in the control, indicating that *Nanog* depletion does not induce precocious cell differentiation. In fact, the expression of *Oct4* mRNA was present in *Nanog*-morphant embryos (Fig. 6D).

To extend our analysis to more markers and confirm the WMISH results, we used RT-PCR analysis of *MO-Nanog* and *OI-Nanog* mRNA injected embryos (Fig. 6E). The RT-PCR results confirmed that the expression levels of differentiation markers associated with early lineage commitment were not significantly changed. Thus, no alterations to the expression of marker genes associated with mesoderm, *Bra*, endoderm, *Sox17* and *FoxA2* [35], nonneural ectoderm, *Gata3* [36] or

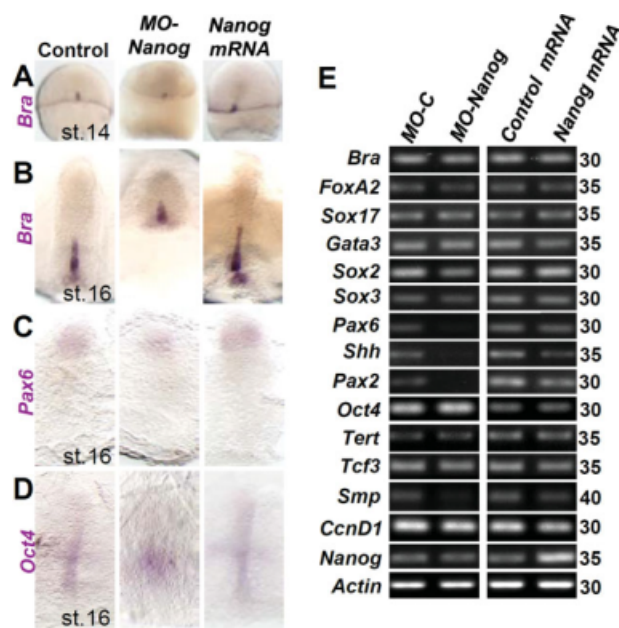


Figure 6. *OI-Nanog* loss or gain of function does not regulate the expression of genes associated with pluripotency or early lineage commitment. (A–D): Analysis of marker expression using whole mount in situ hybridization after *OI-Nanog* depletion or *OI-Nanog* overexpression showing no significant change in the expression pattern of the markers *Bra* (mesoderm; A and B) and *Pax6* (neural ectoderm; C). (D): The expression pattern of *Oct4* (pluripotency) is disorganized but not inhibited. (E): Analysis of the mRNA expression of several markers by reverse-transcriptase polymerase chain reaction on stage 16 embryos. The number of cycles for each amplification is shown on the right.

early neural ectoderm, *Sox2* and *Sox3* [37] were observed. Interestingly, we noted decreased expression of the neural ectoderm marker genes *Pax6*, *Shh* and *Pax2* [34] in *Nanog*-morphant embryos when compared with *MO-C* injected control embryos. These markers are induced in neural ectoderm during the regionalization processes that depend on the interaction between germ layers [38]. Additionally, the expression levels of markers of pluripotency such as *Oct4*, *Tert*, and *Tcf3* [3, 16, 39] were unchanged in *MO-Nanog* and *OI-Nanog* mRNA injected embryos (Fig. 6E). On the other hand, *OI-Nanog* depletion in embryos coincided with a decrease in the expression of *Simplex* (*Smp*), which is homologous to the human *FAM53B* gene and controls cell proliferation in the medaka embryo after the mid-blastula transition (Fig. 6E) [20]. Thus, our results show that *OI-Nanog* does not seem to be necessary for early lineage differentiation and pluripotency.

DISCUSSION

Our study is the first to identify the homologous genes of mammalian *Nanog* in different teleost fish species and to focus on the functional characterization of *Nanog* in medaka. Our results obtained in vivo in medaka suggest that *OI-Nanog* has a primary role in regulating proliferation of ESC, which has been evolutionary conserved among vertebrates [12, 40]. In medaka embryos, *OI-Nanog* expression is maternally inherited and *OI-Nanog* protein has a nuclear expression pattern similar to that of mouse, monkey and human ESCs in culture [41]. Using the medaka fish model, we provide evidence to suggest a role for *OI-Nanog* in controlling proliferation by regulating S-phase transition in the developing vertebrate

embryo. Furthermore, *Ol-Nanog* does not seem to affect early embryonic differentiation or pluripotency maintenance *in vivo*. This is also observed in mice, where *mNanog* does not play an important role in differentiation *in vivo*, but rather modulates stem cell survival and maintenance [12].

In ESC cultures, most cells are in S phase of the cell cycle, with only a few in G1. Activation of *c-Myc* promotes G1-S transition and allows cultures of mESC to self-renew independently of LIF/Stat3 signaling [6], similarly to the effect of *Nanog* overexpression in mESC [1]. In fact, *c-Myc* is one of the necessary factors, along with *Oct4*, *Klf4*, and *Sox2*, to induce pluripotency in somatic cells, highlighting the importance of cell cycle regulation in stemness [6, 42, 43]. Recent experiments in human ESC demonstrate that *NANOG* regulates G1 to S phase transition through direct regulation of *CDC25A* and *CDK6* expression [40]. However, our flow cytometry results using cells from *Ol-Nanog*-depleted embryos demonstrated an increase in the number of cells in S phase and a decrease in the number of cells in G1. Additionally, our qRT-PCR results showed a decrease in *CcnA*, which is required for cell cycle progression through S phase. This suggests that in fish embryos, *Nanog* may regulate S-phase transition or exit. Moreover, *MO-Nanog*-injected embryos demonstrate a decrease in *Smp* expression, which regulates cell cycle in the early embryo [20]. These results suggest that the role of *Ol-Nanog* in cell cycle regulation may be complex and involve several mediator proteins. Nonetheless, in both organisms, human and medaka, *Nanog* seems to regulate the cell cycle at the S-phase level. This further validates medaka as an appropriate model for functional studies of pluripotency genes *in vivo*.

Complete disruption of *Nanog* in mice yields embryos that are composed entirely of disorganized extraembryonic tissues with no discernible epiblast or extra embryonic ectoderm [1]. Similarly, *Ol-Nanog* knockdown medaka embryos do not complete epiboly, but display defects in proliferation with the corresponding morphology of a mass of disorganized large cells. Thus, similar to our observations in medaka, the phenotype in *Nanog*-deficient mice may be a consequence of impaired proliferation; indeed, *Nanog* null mouse blastocysts do not proliferate [1]. However, when the inner cell mass (ICM) from null mutants was cultured *in vitro*, it differentiated only to parietal endoderm-like cells showing its limited differentiation potential [1]. This differs significantly with our results in medaka where, despite the inhibition of proliferation caused by depletion of *Ol-Nanog*, the initial differentiation into the three germ layers proceeds normally in *MO-Nanog*-injected embryos. This difference may be due to the lack of embryonic instructive signals in explanted ICM cells, which may affect the behavior of *Nanog* defective cells *in vitro*.

In medaka, *Ol-Nanog* does not regulate early lineage commitment; however, after *Ol-Nanog* depletion, we observed a decrease in the expression of regionalization markers *Pax6*, *Pax2*, and *Shh*. This result could indicate an effect of *Ol-Nanog* on neural ectoderm regionalization. However, these markers are induced during neural regionalization, which depends on the interaction between the underlying mesoderm and the neural ectoderm. Thus, this result could also be explained by the proliferation defects. The lack of a sufficient number of cells for correct cell migration and morphogenesis may alter mesoderm-ectoderm interactions. This could provoke a regionalization defect and the observed downregulation of *Pax6*, *Pax2*, and *Shh* expression. Thus, the effect of *Nanog* on neural ectoderm regionalization markers needs to be further studied.

Many reports suggest a role for *Nanog* in mammalian ESC differentiation *in vitro* [1, 2, 16, 44–48]. However, in medaka, overexpression of exogenous *Ol-Nanog* or inhibition of endogenous *Ol-Nanog* does not directly affect differentiation. When

cells are explanted outside the embryo, many developmental mechanisms that tightly regulate the correct patterning and differentiation of the whole embryo are not present, which may account for the observed differences in *Nanog* function between *in vitro* and our *in vivo* experiments. In fact, the consequences of manipulating *Nanog* expression levels *in vitro* in ESC vary depending on the levels of *Nanog* and the ESC line used [12, 16, 41, 49]. In any case, *in vitro* studies also show that *Nanog* can be entirely deleted from mESC without eliminating self-renewal or multilineage differentiation potential. Furthermore, chimeras of *mNanog* KO cells in normal mice embryos have demonstrated that *mNanog* KO cells differentiate normally into all tissues, except the gonads, and express *mOct4* [12]. Therefore, these *mNanog* mutant cells are viable, pluripotent, and behave normally in a wild-type embryo. Additionally, *mNanog* null cells expand more slowly than wild-type cells in culture and show a reduction in the total number of stem cell colonies formed [12]. This is in line with our results in medaka, suggesting that *Nanog* plays a major role in regulating proliferation. It will be interesting to test the proliferation capacity of *mNanog* KO cells in chimeric embryos as our experiments predict that this capacity will be compromised *in vivo*. It has previously been proposed that the basic state of pluripotency can be achieved by removing all inducing signals from the media of mESC cultures, suggesting that mESC possess an innate program of self-renewal [50]. In this context, our proposed biological role for *Nanog* during early development would be to regulate embryonic cell proliferation similarly to human ESCs in culture [40].

In mice and chicken, *Nanog* is expressed in the developing gonads [1, 2, 15, 16]. In the present study, we demonstrate that in fish, *Ol-Nanog* is expressed in both male and female gonads, further confirming that *Ol-Nanog* is the functional homolog of mammalian *Nanog*. However, it is not clear whether *Nanog* actually exerts a biological function in gamete maturation or whether it is merely expressed here for future use by the early embryo. In mice chimeric embryos, *mNanog* KO cells never contribute to the adult gonadal tissues, thereby favoring a role for *mNanog* in germ line development [12]. Moreover, human PGC maintain expression of *NANOG* in a small percentage of cells in the fetal testis [51] and *NANOG* is also expressed in human germ cell tumors [52]. In the ovaries, *Ol-Nanog* gene and protein expression are localized in the previtellogenic oocytes but as they mature, the signal diminishes and is undetectable in vitellogenic oocytes. On the other hand, in the testis, *Ol-Nanog* gene expression is detected in the nucleus of cells in the periphery where spermatogonia are located. The expression of *Ol-Nanog* in early gonadal germ cells is similar to *Nanog* expression in mouse and chicken developing gonads [14, 16]. It is noteworthy that *Ol-Nanog* protein expression is detected in the nuclei of peripheral cells where the spermatogonia are located and the cytoplasm of cells within cysts where spermatogenesis occurs in the medaka testes. In addition, *Ol-Nanog* expression patterns in the adult gonads of medaka are similar to those observed for the *Ovas* gene, the homolog of *Vasa* which is expressed specifically in the PGCs and is necessary for gonad development [53]. Thus, *Ol-Nanog* gene and protein expression in both male and female gonads suggest a specific role for *Ol-Nanog* in gamete development.

CONCLUSION

We have identified *Nanog* homologs in various species and functionally characterized the medaka *Nanog* homolog during embryonic development. *Ol-Nanog* is expressed in embryos up to stage 20 when it is downregulated. Later in development, it can be detected after hatching at the fry stage and in the adult

male and female gonads. Our *in vivo* functional analysis demonstrates that *Ol-Nanog* is necessary for proliferation during early embryo development and regulates S-phase transition without affecting early lineage commitment. Together, these findings describe developmental functions of *Nanog* in regulating proliferation during fish embryonic development and support other studies which demonstrate that Nanog is not a critical factor underlying regulation of differentiation *in vivo*. They also introduce the medaka fish as a valid model for functional studies of pluripotency genes.

ACKNOWLEDGMENTS

We thank M. Scharlt, P. Bovolenta, T. Czerny, and Y. Wakamatsu for help with medaka and reagents; and M. Lako, D.

Burks, and P. Sánchez for discussions and critical reading of the manuscript. This work was supported by grants from the Spanish Ministerio de Educación y Ciencia (BFU2005-09186), the Spanish Instituto de Salud Carlos III, and the Valencian Health Council (GV05/221 and ACOMP06/145) to J.L.M. and Spanish ISCIII FIS 02/303 and PI07/0789 to A.G.-E. L.O. is currently affiliated with Centro Nacional de Investigaciones Oncológicas, Madrid, Spain.

DISCLOSURE OF POTENTIAL CONFLICTS OF INTEREST

The authors indicate no potential conflicts of interest.

REFERENCES

- Mitsui K, Tokuzawa Y, Itoh H et al. The homeoprotein Nanog is required for maintenance of pluripotency in mouse epiblast and ES cells. *Cell* 2003;113:631–642.
- Chambers I, Colby D, Robertson M et al. Functional expression cloning of Nanog, a pluripotency sustaining factor in embryonic stem cells. *Cell* 2003;113:643–655.
- Nichols J, Zevnik B, Anastasiadis K et al. Formation of pluripotent stem cells in the mammalian embryo depends on the POU transcription factor Oct4. *Cell* 1998;95:379–391.
- Avilion AA, Nicolis SK, Pevny LH et al. Multipotent cell lineages in early mouse development depend on SOX2 function. *Genes Dev* 2003;17:126–140.
- Orkin SH. Chipping away at the embryonic stem cell network. *Cell* 2005;122:828–830.
- Burdon T, Smith A, Savatier P. Signalling, cell cycle and pluripotency in embryonic stem cells. *Trends Cell Biol* 2002;12:432–438.
- Hanna LA, Foreman RK, Tarasenko IA et al. Requirement for Foxd3 in maintaining pluripotent cells of the early mouse embryo. *Genes Dev* 2002;16:2650–2661.
- Sakaki-Yumoto M, Kobayashi C, Sato A et al. The murine homolog of SALL4, a causative gene in Okihiro syndrome, is essential for embryonic stem cell proliferation, and cooperates with Sall1 in anorectal, heart, brain and kidney development. *Development* 2006;133:3005–3013.
- Wu Q, Chen X, Zhang J et al. Sall4 interacts with Nanog and co-occupies Nanog genomic sites in embryonic stem cells. *J Biol Chem* 2006;281:24090–24094.
- Zhang J, Tam WL, Tong GQ et al. Sall4 modulates embryonic stem cell pluripotency and early embryonic development by the transcriptional regulation of Pou5f1. *Nat Cell Biol* 2006;8:1114–1123.
- Niakan KK, Davis EC, Clipsham RC et al. Novel role for the orphan nuclear receptor Dax1 in embryogenesis, different from steroidogenesis. *Mol Genet Metab* 2006;88:261–271.
- Chambers I, Silva J, Colby D et al. Nanog safeguards pluripotency and mediates germline development. *Nature* 2007;450:1230–1234.
- Silva J, Chambers I, Pollard S et al. Nanog promotes transfer of pluripotency after cell fusion. *Nature* 2006;441:997–1001.
- Yamaguchi S, Kimura H, Tada M et al. Nanog expression in mouse germ cell development. *Gene Expr Patterns* 2005;5:639–646.
- Cañón S, Herranz C, Manzanares M. Germ cell restricted expression of chick Nanog. *Dev Dyn* 2006;235:2889–2894.
- Lavial F, Acloque H, Bertocchini F et al. The Oct4 homolog PouV and Nanog regulate pluripotency in chicken embryonic stem cells. *Development* 2007;134:3549–3563.
- Morrison GM, Brickman JM. Conserved roles for Oct4 homologs in maintaining multipotency during early vertebrate development. *Development* 2006;133:2011–2022.
- Sun L, Bradford CS, Ghosh C, et al. ES-like cell cultures derived from early zebrafish embryos. *Mol Mar Biol Biotechnol* 1995;4:193–199.
- Hong Y, Winkler C, Scharlt M. Pluripotency and differentiation of embryonic stem cell lines from the medakafish (*Oryzias latipes*). *Mech Dev* 1996;60:33–44.
- Thermes V, Candal E, Alunni A et al. Medaka simplot (FAM53B) belongs to a family of novel vertebrate genes controlling cell proliferation. *Development* 2006;133:1881–1890.
- Burgess S, Reim G, Chen W, et al. The zebrafish *spiel-ohne-grenzen* (*spg*) gene encodes the POU domain protein Pou2 related to mammalian Oct4 and is essential for formation of the midbrain and hindbrain, and for pre-gastrula morphogenesis. *Development* 2002;129:905–916.
- Hong Y, Winkler C, Liu T, et al. Activation of the mouse Oct4 promoter in medaka embryonic stem cells and its use for ablation of spontaneous differentiation. *Mech Dev* 2004;121:933–943.
- Yamamoto T, ed. *Medaka (Killifish): Biology and Strains*. Tokyo: Heigaku Publishing, 1975.
- Iwamatsu T. Stages of normal development in the medaka *Oryzias latipes*. *Mech Dev* 2004;121:605–618.
- Sarkar IN, Thornton JW, Planet PJ et al. An automated phylogenetic key for classifying homeoboxes. *Mol Phylogenet Evol* 2002;24:388–399.
- Swofford DL. *PAUP*: Phylogenetic Analysis Using Parsimony (and Other Methods)*. Sunderland, MA: Sinauer, 2000.
- Aguilar D, Bustos M, Caracuel MD. Coloraciones histopatológicas rutinarias de mayor interés. In: García del Moral R, ed. *Laboratorio de Anatomía Patológica*. Madrid: McGraw Hill Interamericana de España, 1993:155–174.
- Loosli F, Köster RW, Carl M et al. Six3, a medaka homolog of the Drosophila homeobox gene *sine oculis* is expressed in the anterior embryonic shield and the developing eye. *Mech Dev* 1998;74:159–164.
- García-España A, Chung PJ, Sarkar IN et al. Appearance of new tetraspanin genes during vertebrate evolution. *Genomics* 2008;91:326–334.
- Jauch R, Ng CK, Saikatendu KS, et al. Crystal structure and DNA binding of the homeodomain of the stem cell transcription factor Nanog. *J Mol Biol* 2008;376:758–770.
- Kasahara M, Naruse K, Sasaki S et al. The medaka draft genome and insights into vertebrate genome evolution. *Nature* 2007;447:714–719.
- Chiu JC, Lee EK, Egan MG et al. OrthologID: automation of genome-scale ortholog identification within a parsimony framework. *Bioinformatics* 2006;22:699–707.
- Smith JC, Price BM, Green JB et al. Expression of a *Xenopus* homolog of Brachyury (T) is an immediate-early response to mesoderm induction. *Cell* 1991;67:79–87.
- Stoykova A, Gruss P. Roles of Pax-genes in developing and adult brain as suggested by expression patterns. *J Neurosci* 1994;14:1395–1412.
- Sinner D, Rankin S, Lee M et al. Sox17 and β catenin cooperate to regulate the transcription of endodermal genes. *Development* 2004;131:3069–3080.
- Sheng G, Stern CD. Gata2 and Gata3: novel markers for early embryonic polarity and for non-neural ectoderm in the chick embryo. *Mech Dev* 1999;87:213–216.
- Uwanogho D, Rex M, Cartwright EJ et al. Embryonic expression of the chicken Sox2, Sox3 and Sox11 genes suggests an interactive role in neuronal development. *Mech Dev* 1995;49:23–36.
- Lupo G, Harris WA, Lewis KE. Mechanisms of ventral patterning in the vertebrate nervous system. *Nat Rev Neurosci* 2006;7:103–114.
- Pereira L, Yi F, Merrill BJ. Repression of Nanog gene transcription by Tcf3 limits embryonic stem cell self-renewal. *Mol Cell Biol* 2006;26:7479–7491.
- Zhang X, Neganova I, Przyborski S, et al. A role for NANOG in G1 to S transition in human embryonic stem cells through direct binding of CDK6 and CDC25A. *J Cell Biol* 2009;184:67–82.
- Hatano SY, Tada M, Kimura H et al. Pluripotential competence of cells associated with Nanog activity. *Mech Dev* 2005;122:67–79.

- 42 Takahashi K, Yamanaka S. Induction of pluripotent stem cells from mouse embryonic and adult fibroblast cultures by defined factors. *Cell* 2006;126:663–676.
- 43 Takahashi K, Tanabe K, Ohnuki M et al. Induction of pluripotent stem cells from adult human fibroblasts by defined factors. *Cell* 2007; 131:861–872.
- 44 Boyer LA, Lee TI, Cole MF et al. Core transcriptional regulatory circuitry in human embryonic stem cells. *Cell* 2005;122: 947–956.
- 45 Ivanova N, Dobrin R, Lu R et al. Dissecting self-renewal in stem cells with RNA interference. *Nature* 2006;442:533–538.
- 46 Loh YH, Wu Q, Chew JL et al. The Oct4 and Nanog transcription network regulates pluripotency in mouse embryonic stem cells. *Nat Genet* 2006;38:431–440.
- 47 Wang J, Rao S, Chu J et al. A protein interaction network for pluripotency of embryonic stem cells. *Nature* 2006;444:364–368.
- 48 Hyslop L, Stojkovic M, Armstrong L et al. Downregulation of NANOG induces differentiation of human embryonic stem cells to extraembryonic lineages. *Stem Cells* 2005;23:1035–1043.
- 49 Darr H, Maysnar Y, Benvenisty N. Overexpression of NANOG in human ES cells enables feeder-free growth while inducing primitive ectoderm features. *Development* 2006;133:1193–1201.
- 50 Ying QL, Wray J, Nichols J et al. The ground state of embryonic stem cell self-renewal. *Nature* 2008;453:519–523.
- 51 Kerr CL, Hill CM, Blumenthal PD et al. Expression of pluripotent stem cell markers in the human fetal testis. *Stem Cells* 2008;26:412–421.
- 52 Hart AH, Hartley L, Parker K et al. The pluripotency homeobox gene NANOG is expressed in human germ cell tumors. *Cancer* 2005;15:2092–2098.
- 53 Shinomiya A, Tanaka M, Kobayashi T et al. The vasa-like gene, olvas, identifies the migration path of primordial germ cells during embryonic body formation stage in the medaka, *Oryzias Latipes* *Dev Growth Differ* 2000;42:317–326.



See www.StemCells.com for supporting information available online.